

**Capacity of unreinforced masonry walls in out-of-plane two-way bending  
A review of analytical formulations**

Chang, Lang-Zhi; Messali, Francesco; Esposito, Rita

**DOI**

[10.1016/j.istruc.2020.10.060](https://doi.org/10.1016/j.istruc.2020.10.060)

**Publication date**

2020

**Document Version**

Final published version

**Published in**

Structures

**Citation (APA)**

Chang, L.-Z., Messali, F., & Esposito, R. (2020). Capacity of unreinforced masonry walls in out-of-plane two-way bending: A review of analytical formulations. *Structures*, 28, 2431-2447.  
<https://doi.org/10.1016/j.istruc.2020.10.060>

**Important note**

To cite this publication, please use the final published version (if applicable).  
Please check the document version above.

**Copyright**

Other than for strictly personal use, it is not permitted to download, forward or distribute the text or part of it, without the consent of the author(s) and/or copyright holder(s), unless the work is under an open content license such as Creative Commons.

**Takedown policy**

Please contact us and provide details if you believe this document breaches copyrights.  
We will remove access to the work immediately and investigate your claim.



# Capacity of unreinforced masonry walls in out-of-plane two-way bending: A review of analytical formulations

Lang-Zi Chang (常浪子)\*, Francesco Messali, Rita Esposito

Faculty of Civil Engineering and Geosciences, Delft University of Technology, Stevinweg 1, 2628 CN Delft, The Netherlands

## ARTICLE INFO

### Keywords:

Unreinforced masonry  
Out-of-plane  
Two-way bending  
Analytical formulations  
Crucial factors  
Sensitivity studies

## ABSTRACT

Investigations of post-seismic events show that the collapse of walls in out-of-plane (OOP) two-way bending can be one of the most predominant failure mechanisms for unreinforced masonry (URM) structures. To assess the force capacity of URM walls in OOP two-way bending, various analytical formulations have been developed during past decades. However, the accuracy and the application range of these analytical formulations have been evaluated against only a limited number of experiments. For this purpose, a dataset of 46 testing specimens from 8 international testing campaigns was created and used to evaluate current analytical formulations, namely Eurocode 6 based on the yield line method, Australian Standard AS3700 based on the virtual work method, and two other virtual work formulations related to AS3700. A general comparison shows that within the listed dataset, AS3700 overall provides the most accurate predictions. More specifically, AS3700 is the most accurate assessing walls assumed to be partially clamped and walls with openings. Testing specimens were divided into groups to study the influence of crucial factors, such as material properties, boundary conditions, pre-compression, aspect ratio and openings. However, only in a few cases clear trends were identified from the testing data. Sensitivity studies were carried out to reveal how the analytical formulations assess the influence of the crucial factors on the force capacity of the walls. Results expose drawbacks and limitations of the considered analytical formulations. Eventually, potential directions for improving the accuracy and the application range of the analytical formulations are pointed out.

## 1. Introduction

Research shows that the out-of-plane (OOP) failure of structural components can be one of the most predominant failure mechanisms in unreinforced masonry (URM) buildings [1–4]. Various analytical formulations have been developed during past decades to assess the force capacity of URM walls. Compared with one-way vertically spanning walls, for which analytical formulations have been well developed [5–8], analytical formulations for URM walls in OOP two-way bending require further improvement in accuracy and extension for the application range.

To improve the understanding of URM walls in OOP two-way bending, testing campaigns have been carried out worldwide. Chong [9], van der Pluijm [10,11] and Derakhshan et al. [12] performed monotonic pushover tests to determine the force capacity of walls. Besides, walls subjected to quasi-static cyclic OOP loading have been tested to determine their post-peak behaviour and energy dissipation [13–18]. Shake table tests have also been conducted by Vaculik and Griffith [19]

and Graziotti et al. [20] to observe the wall behaviour under dynamic loading. Several testing campaigns have been used to evaluate the accuracy of the analytical formulations [12,20,21], even though each campaign has a limited number of testing samples. Furthermore, research on the crucial factors to which the force capacity of walls can be sensitive, such as boundary conditions, is limited to only a few testing samples. This poses limitations in validating and developing current analytical formulations.

Analytical formulations have been developed in past decades and incorporated in standards to assess the wall capacity in engineering practice. Current analytical formulations are mainly based on the yield line method or on the virtual work method. The yield line method by Haseltine et al. [22], together with its variations, such as the fracture line method by Sinha [23] and Hendry et al. [24], contributed to the method currently proposed in Eurocode 6 [25]. The core concepts of the yield line method are: masonry is simplified as a homogeneous material; all cracks develop simultaneously; the force capacity is calculated from the equilibrium between the applied forces and the reaction forces along cracking lines. One drawback of the yield line method is that some

\* Corresponding author.

E-mail addresses: [L.Chang-2@tudelft.nl](mailto:L.Chang-2@tudelft.nl) (L.-Z. Chang), [F.Messali@tudelft.nl](mailto:F.Messali@tudelft.nl) (F. Messali), [R.Esposito@tudelft.nl](mailto:R.Esposito@tudelft.nl) (R. Esposito).

Nomenclature			
$f_{bt}$	the flexural strength of the masonry unit	$R_{f,H}$	the restraint factor with regard to horizontal boundaries
$f_{x1}$	the flexural strength of masonry having failure plane parallel to bed joints, here named vertical flexural strength	$s_p$	the minimum overlap of masonry units in successive courses
$f_{x2}$	the flexural strength of masonry having failure plane perpendicular to bed joints, here named horizontal flexural strength	$t_j$	the thickness of mortar joint
$G$	the assumed slope of the crack line	$t_u$	the masonry unit thickness
$H_0$	the height of the opening	$t_w$	the wall thickness
$H_d$	the design height of the wall	$w$	the force capacity
$H_d'$	the calibrated design height of the wall	$x$	the distance between the central line of the wall and that of the opening
$h_u$	the height of the masonry unit	$Z$	the section modulus of the wall
$H_w$	the height of the wall	$Z_d$	the section modulus of the bedded area
$k_1, k_2$	coefficients to assess lateral load capacity	$Z_p$	the lateral section modulus based on the mortar contact area of the perpend joints
$k_b$	a coefficient for computing the torsional shear capacity of the bed joints	$Z_t$	the equivalent torsional section modulus
$k_p$	the perpend spacing factor	$Z_u$	the lateral section modulus of the masonry units
$L_0$	the length of the opening	$\alpha$	the slope factor
$L_d$	the design length of the wall	$\alpha_2$	the bending moment coefficient
$l_u$	the length of the masonry unit	$\alpha_f$	an aspect factor
$L_w$	the length of the wall	$\eta$	the normalised length of the opening
$M_d$	the diagonal bending moment capacity	$\lambda$	the normalised eccentricity of the opening
$M_h$	the horizontal bending moment capacity	$\mu$	the flexural strength ratio
$n$	the number of layers counted between the wall corner and the closest starting point of the diagonal crack	$\nu$	the Poisson's ratio
$R_f$	the restraint factor with regard to vertical boundaries	$\sigma$	the pre-compression
		$\sigma_d$	the vertical compressive stress at specific height of the wall
		$\tau_u$	the ultimate torsional shear strength of masonry
		$\varphi$	the capacity reduction factor
		$\phi$	the tangent of the assumed slope of the crack line $G$

crucial factors such as bonding patterns are neglected since masonry is considered as a homogenous material. This can affect the crack pattern therefore possibly resulting in misevaluation. Another drawback of the yield line method is that all cracks are assumed to develop concurrently, which can lead to inaccuracy for calculating the force capacity since contributions of all cracks are taken into account. However, some tests suggest that cracks develop in sequence and a central horizontal crack may not contribute to the force capacity [13–15]. Although Eurocode 6 recommends in general the use of the yield line theory, it provides guidance to define the value of the coefficients needed in the formulations only for a limited number of cases presented in the informative Annex E. There, the boundary conditions of the walls are considered as either hinged or clamped (an intermediate status is not covered), and the openings are not taken into account.

Another category of analytical formulations originates from the virtual work method. Lawrence and Marshall [26] firstly applied the virtual work method to evaluate the force capacity of URM walls in two-way bending, and later it was adopted by the Australian Standard AS3700 [27], though the formulas for moment capacity are empirical and in some cases dimensionally inconsistent. Willis et al. [28] refined the method by calculating bending moment capacity based on theoretical derivation rather than on empirical formulas as in AS3700. Graziotti et al. [20] adopted the same theoretical framework by Willis et al. [28] and experimentally evaluated the torsional strength to avoid the misleading influence of the flexural strength of masonry on the torsional strength. However, new theoretical formulations were not proposed. Furthermore, Derakhshan et al. [12] modified the virtual work method to include the effects of plaster. The core concepts of the virtual work method are: the contributions from horizontal cracks are neglected; diagonal cracks start right from the wall corners; the cracking pattern is assumed to follow the mortar joints and is determined by the aspect ratios of the units and of the wall; horizontal and diagonal bending moment capacities are calculated independently; the virtual work done by external loads is equal to the strain energy along cracking lines in pre-assumed cracking patterns (Fig. 1). Additionally, the virtual work

method provides coefficients and formulas to consider the presence of openings. However, some limitations still exist. One limitation is related to the restraint factor  $R_f$  that is used to evaluate the rotational stiffness of the vertical boundary conditions. Although some researchers including Griffith and Vaculik [21], suggest that  $R_f$  can be taken as 0.5 for partially clamped walls (walls that are neither hinged or clamped but have a finite rotational stiffness), such as walls with return walls, this cannot be generalised for other forms of boundary conditions. Moreover, the application range of AS3700 formulations is limited to single-wythe walls built in stretcher bond.

The afore-mentioned formulations are all force-based methods. In recent years, displacement-based methods have also been developed. Vaculik and Griffith [29] proposed a displacement-based method to estimate the complete force–displacement relationship of walls. This displacement-based method neglects the contribution given by the flexural strength of masonry and is only suitable for application in the post-peak response of URM walls under two-way bending, which results in a substantial underestimation of the force capacity. Besides, the application of this formulation is currently limited to a few predefined failure mechanisms.

Based on the discussion above, it can be concluded that much progress has been made, but a number of drawbacks and limitations still lie within current analytical formulations. Consequently, it is worthy to evaluate the accuracy and application range of these formulations and identify directions to improve them. This paper aims at evaluating the accuracy and application range of four force-based analytical formulations proposed by Eurocode 6 (EC6) [25], Australian Standard (AS3700) [27], Willis et al. (W2006) [28] and Graziotti et al. (G2019) [20]. For this purpose, 46 testing specimens from 8 international testing campaigns on URM walls in OOP two-way bending were collected and categorised (Section 2); analytical predictions were compared with the testing results to evaluate the accuracy of the analytical formulations (Section 3); the testing specimens were divided into groups to assess the influence of crucial factors on the force capacity in tests; sensitivity studies were carried out to evaluate whether the influence of the crucial

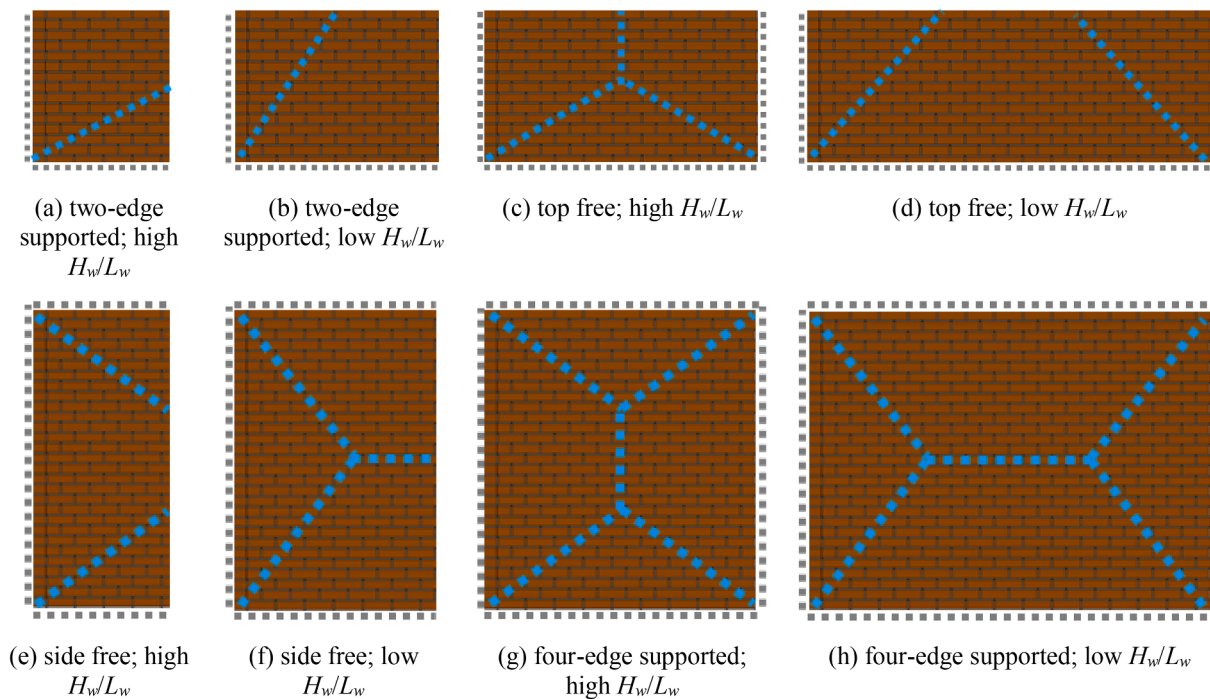


Fig. 1. Classic pre-assumed cracking patterns used in formulations based on the virtual work method (adapted from [12]).

factors predicted by the analytical formulations matches with that revealed by the testing results (Section 4). Eventually, potential directions for improving the accuracy and application range of the analytical formulations are pointed out (Section 5).

## 2. Research methodology

### 2.1. Selection of the testing specimens

A dataset of 46 testing specimens from 8 international testing campaigns in recent 30 years on URM walls in OOP two-way bending was created. Earlier testing campaigns were not included in this paper due to the unavailability of the complete testing data. Table 1 lists the characteristics of all the selected testing specimens [9–14,16–20]. The dataset consists of tests performed mostly on clay brick and calcium silicate (CS) brick masonry walls. 37 out of 46 testing specimens were subjected to quasi-static cyclic loading, while the others to dynamic loading. Only 5 testing specimens were made in half-scale. Over half of the walls were supported on four edges, namely “O” shaped walls; 1/3 of the walls were unsupported at the top edge, i.e. “U” shaped walls; only 4 walls were unsupported on one vertical edge, i.e. “C” shaped walls. Vertical supports constructed with return walls to simulate partially clamped edges were in nearly half of the testing specimens. Only less than half of the walls were tested under pre-compression, even though in practice most walls are vertically load-bearing. With regard to aspect ratio, all walls were tested with a height to length ratio lower than unity ( $H_w/L_w \leq 1$ ). Approximately 50% of the testing specimens had openings. In the majority of the cases, the walls were single-wythe and built with stretcher bond; only 2 walls were double-wythe and built in English bond.

### 2.2. Analytical formulations considered

Fig. 2 shows the testing configuration with the adopted terminology used to describe the testing specimens.  $H_w$  and  $L_w$  are the height and the length of the wall, respectively;  $H_0$  and  $L_0$  are the height and the length of the opening, respectively;  $x$  is the distance between the centre line of the opening and that of the wall;  $h_u$ ,  $l_u$  and  $t_u$  are the height, the length

and the thickness of masonry units, respectively;  $t_j$  is the thickness of the mortar joints. The red dotted lines denote presupposed diagonal cracking patterns in the virtual work method.

Four groups of analytical formulations, namely Eurocode 6 (EC6) [25], AS3700 [27], Willis et al. (W2006) [28] and Graziotti et al. (G2019) [20] were compared to evaluate the force capacity of above-mentioned testing specimens. The recently developed displacement-based seismic design method presented in [29] was not considered due to the fact that it mainly focuses on the determination of the force–displacement relationship, and it neglects the contribution of the flexural strength of masonry. In this sense it generally results in an over-conservative prediction on the force capacity.

EC6 evaluates the force capacity  $w$  of a wall by following equation:

$$w = \frac{(f_{x1} + \sigma_d)Z}{\mu\alpha_2 L_w^2} \tag{1}$$

where the flexural strength ratio  $\mu$  is defined as:

$$\mu = (f_{x1} + \sigma_d)/f_{x2} \tag{2}$$

with  $f_{x1}$  and  $f_{x2}$  being the flexural strength of masonry obtained for planes of failure parallel to and perpendicular to the bed joints, respectively;  $\sigma_d$  is the vertical compressive stress at specific height of the wall caused by self-weight and pre-compression  $\sigma$ ;  $Z$  is the section modulus of the wall;  $\alpha_2$  is the bending moment coefficient. In this work, the values of  $\alpha_2$ , which is allowed to be obtained from a suitable theory, were taken from the Annex E of EC6, where  $\alpha_2$  is provided as a dependent variable of  $\mu$ ,  $H_w/L_w$  and boundary conditions in tabular form.

The formulations AS3700, W2006 and G2019 assess the force capacity  $w$  of a wall by the following equation:

$$w = \frac{2\alpha_f}{L_d^2} (k_1 M_h + k_2 M_d) \tag{3}$$

with the components of Eq. (3):

$$G = \frac{2(h_u + t_j)}{l_u + t_j} \tag{4}$$

**Table 1**  
Dataset of URM walls in OOP two-way bending.

Testing campaigns	Testing specimens	Presence of opening#	Supporting types*	Unit type	Bonding pattern	Geometry					Pre-compression		Material properties			Testing results	
						Unit geometry	Joint thickness	Wall geometry	Aspect ratio	Opening	Masonry density	Pre-compression	Flexural strength of				
													$l_u \times h_u \times t_u$ (mm <sup>3</sup> )	$t_j$ (mm)	$L_w \times H_w \times t_w$ (mm <sup>3</sup> )		$H_w/L_w$
						$f_{x1}$ (MPa)	$f_{x2}$ (MPa)	$f_{bt}$ (MPa)	$w$ (kPa)								
Chong (1993), full scale quasi-static	SB01	No	U	Clay	Stretcher	215 × 65 × 102.5	14	5615 × 2475 × 102.5	0.44	–	–	15.15	0	0.47	1.67	3.82	2.80
	SB02	Yes(C)	U	Clay	Stretcher	215 × 65 × 102.5	14	5615 × 2475 × 102.5	0.44	2260	0	15.15	0	0.47	1.67	3.82	2.40
	SB03	Yes(C)	U	Clay	Stretcher	215 × 65 × 102.5	14	5615 × 2475 × 102.5	0.44	2935	0	15.15	0	0.47	1.67	3.82	2.30
	SB04	Yes(C)	U	Clay	Stretcher	215 × 65 × 102.5	14	5615 × 2475 × 102.5	0.44	910 × 1125	0	15.15	0	0.47	1.67	3.82	2.20
	SB05	No	U	Clay	Stretcher	215 × 65 × 102.5	14	5615 × 2475 × 102.5	0.44	–	–	15.15	0	0.47	1.67	3.82	2.70
	SB06	No	O	Clay	Stretcher	215 × 65 × 102.5	14	2900 × 2450 × 102.5	0.84	–	–	15.15	0	0.47	1.67	3.82	7.50
	SB07	Yes(C)	O	Clay	Stretcher	215 × 65 × 102.5	14	2900 × 2450 × 102.5	0.84	900 × 900	0	15.15	0	0.47	1.67	3.82	5.50
	SB09	Yes(E)	U(re)	Clay	Stretcher	215 × 65 × 102.5	14	5615 × 2475 × 102.5	0.44	900 × 900	1457.5	15.15	0	0.47	1.67	3.82	2.40
	DC01	No	U	Concrete	Stretcher	440 × 215 × 100	14	5615 × 2475 × 100	0.44	–	–	19.61	0	1.37	1.68	1.20	2.65
	DC02	Yes(C)	U	Concrete	Stretcher	440 × 215 × 100	14	5615 × 2475 × 100	0.44	2260	0	19.61	0	1.37	1.68	1.20	1.75
DC02B	Yes(C)	U	Concrete	Stretcher	440 × 215 × 100	14	5615 × 2475 × 100	0.44	2260 × 1125	0	19.61	0	1.37	1.68	1.20	1.50	
HW01	No	C	Clay	Stretcher	215 × 65 × 102.5	10	2700 × 2475 × 102.5	0.92	–	–	28.84	0	0.77	4.12	13.09	3.70	
HW02	Yes(E)	C	Clay	Stretcher	215 × 65 × 102.5	10	2700 × 2475 × 102.5	0.92	460 × 535	110	28.84	0	0.77	4.12	13.09	2.80	
HW03	Yes(C)	C	Clay	Stretcher	215 × 65 × 102.5	10	2700 × 2475 × 102.5	0.92	460 × 1150	0	28.84	0	0.77	4.12	13.09	3.30	
HW04	Yes(C)	C	Clay	Stretcher	215 × 65 × 102.5	10	2700 × 2475 × 102.5	0.92	900 × 535	0	28.84	0	0.77	4.12	13.09	3.70	
W01	Yes(C)	U	Clay	Stretcher	215 × 65 × 102.5	10	5615 × 2475 × 102.5	0.44	340 × 235	0	28.84	0	0.77	4.12	13.09	2.30	
van der Pluijm (1999, 2001), full scale quasi-static	Panel II	No	O	Clay	Stretcher	204 × 50 × 98	10	3949 × 1738 × 98	0.44	–	–	18.18	0	0.26	1.52	4.04	4.41
	CS-b panel	No	O	CS	Stretcher	437 × 198 × 100	2	3960 × 1800 × 100	0.45	–	–	17.50	0	0.68	1.22	1.89	5.60
	CS-e panel	No	O	CS	Stretcher	897 × 598 × 100	2	3960 × 1800 × 100	0.45	–	–	17.50	0	0.66	1.05	1.54	5.59
	sm-RLJ panel	No	O	Clay	Stretcher	206 × 50 × 96	2	3990 × 1800 × 96	0.45	–	–	11.55	0	1.03	1.77	2.70	5.52
Griffith et al. (2007), full scale quasi-static cyclic	Wall 1	No	O(re)	Clay	Stretcher	230 × 76 × 110	10	4080 × 2494 × 110	0.61	–	–	19.00	0.1	0.61	1.92	3.55	4.76
	Wall 2	No	O(re)	Clay	Stretcher	230 × 76 × 110	10	4080 × 2494 × 110	0.61	–	–	19.00	0	0.61	1.92	3.55	3.04
	Wall 3	Yes(E)	O(re)	Clay	Stretcher	230 × 76 × 110	10	4080 × 2494 × 110	0.61	1200 × 1000	780	19.00	0.1	0.61	1.92	3.55	5.05
	Wall 4	Yes(E)	O(re)	Clay	Stretcher	230 × 76 × 110	10	4080 × 2494 × 110	0.61	1200 × 1000	780	19.00	0.05	0.61	1.92	3.55	3.91
	Wall 5	Yes(E)	O(re)	Clay	Stretcher	230 × 76 × 110	10	4080 × 2494 × 110	0.61	1200 × 1000	780	19.00	0	0.61	1.92	3.55	3.59
	Wall 6	Yes(E)	U(re)	Clay	Stretcher	230 × 76 × 110	10	4080 × 2494 × 110	0.61	1200 × 946	780	19.00	0	0.61	1.92	3.55	1.97
	Wall 7	Yes(C)	O(re)	Clay	Stretcher	230 × 76 × 110	10	2520 × 2494 × 110	0.99	1200 × 946	0	19.00	0.1	0.61	1.92	3.55	8.71
	Wall 8	Yes(C)	O(re)	Clay	Stretcher	230 × 76 × 110	10	2520 × 2494 × 110	0.99	1200 × 946	0	19.00	0	0.61	1.92	3.55	8.52
		No	O	Clay	Stretcher	212 × 50 × 102	10	4000 × 2751 × 102	0.69	–	–	16.00	0.06	0.38	1.18	4.78	3.61

(continued on next page)

Table 1 (continued)

Testing campaigns	Testing specimens	Presence of opening#	Supporting types*	Unit type	Bonding pattern	Geometry						Pre-compression		Material properties			Testing results	
						Unit geometry		Wall geometry		Aspect ratio	Opening		Masonry density	Pre-compression	Flexural strength of			
						$l_u \times h_u \times t_u$ (mm <sup>3</sup> )	$t_j$ (mm)	$L_w \times H_w \times t_w$ (mm <sup>3</sup> )	$H_w/L_w$		$L_o \times H_o$ (mm <sup>2</sup> )	$x$ (mm)			Masonry			Unit
										$\gamma$ (kN/m <sup>3</sup> )			$\sigma$ (MPa)	$f_{x1}$ (MPa)	$f_{x2}$ (MPa)	$f_{bt}$ (MPa)		
Messali et al. (2017); Damiola et al. (2018), full scale quasi-static cyclic	TUD_COMP-10	No	O	CS	Stretcher	212 × 71 × 102	10	3986 × 2765 × 102	0.69	–	–	17.50	0.06	0.26	0.55	2.74	2.45	
	TUD_COMP-11	Yes(E)	O	CS	Stretcher	212 × 71 × 102	10	3986 × 2765 × 102	0.69	1776 × 1640	449	17.50	0.06	0.26	0.55	2.74	3.67	
	TUD_COMP-12	No	O	Clay	Stretcher	210 × 50 × 100	10	3950 × 2710 × 100	0.69	–	–	16.50	0.06	0.16	0.65	6.31	3.37	
	TUD_COMP-26	No	O	Clay	English	210 × 50 × 100	10	3840 × 2710 × 210	0.71	–	–	16.50	0.06	0.14	0.41	6.31	7.52	
Vaculik et al. (2018), half scale dynamic	d1	No	O(re)	Clay	Stretcher	110 × 39 × 50	5	1840 × 1232 × 50	0.67	–	–	21.20	0.1	0.42	1.30	2.40	3.95	
	d2	No	O(re)	Clay	Stretcher	110 × 39 × 50	5	1840 × 1232 × 50	0.67	–	–	21.20	0	0.42	1.30	2.40	2.47	
	d3	Yes(E)	O(re)	Clay	Stretcher	110 × 39 × 50	5	1840 × 1232 × 50	0.67	575 × 528	316.5	21.20	0.1	0.42	1.30	2.40	2.67	
	d4	Yes(E)	O(re)	Clay	Stretcher	110 × 39 × 50	5	1840 × 1232 × 50	0.67	575 × 528	316.5	21.20	0.05	0.42	1.30	2.40	2.65	
	d5	Yes(E)	O(re)	Clay	Stretcher	110 × 39 × 50	5	1840 × 1232 × 50	0.67	575 × 528	316.5	21.20	0	0.42	1.30	2.40	1.61	
Derakhshan et al. (2018), full scale quasi-static	A-3	No	O(re)	Clay	Stretcher	230 × 110 × 76	10	3020 × 2750 × 76	0.91	–	–	19.00	0.008	0.15	0.47	0.87	1.9	
	B-3	No	O(re)	Clay	Stretcher	230 × 110 × 76	10	3260 × 2720 × 76	0.83	–	–	19.00	0.008	0.15	0.47	0.87	1.71	
	B-5	No	O(re)	Clay	Stretcher	230 × 110 × 76	10	3040 × 2720 × 76	0.89	–	–	19.00	0.008	0.15	0.47	0.87	2.37	
Graziotti et al. (2019), full scale dynamic	CS-005-RR	No	O(re)	CS	Stretcher	212 × 71 × 102	10	3980 × 2750 × 102	0.69	–	–	18.05	0.05	0.95	1.29	2.61	3.70	
	CS-000-RF	No	U(re)	CS	Stretcher	212 × 71 × 102	10	3980 × 2750 × 102	0.69	–	–	18.05	0.00	0.95	1.29	2.61	2.65	
	CSW-000-RF	Yes(E)	U(re)	CS	Stretcher	212 × 71 × 102	10	3980 × 2750 × 102	0.69	1790 × 1630	445	18.05	0.00	0.95	1.29	2.61	2.34	
	CL-000-RF	No	U(re)	Clay	Stretcher	208 × 50 × 98	10	4020 × 2760 × 98	0.69	–	–	19.63	0.00	0.41	1.98	7.83	3.30	
Padalu et al. (2020), full scale quasi-static cyclic	URM-F	No	O(re)	Clay	English	229 × 72 × 109	10	3000 × 3000 × 229	1	–	–	19.00	0.125	0.45	0.46	2.60	19.26	

# Yes(C) and Yes(E) denote that the opening is centrally and eccentrically located, respectively.

\* “U” shape: the top of the wall is free; “C” shape: one vertical edge of the wall is free; “O” shape: all edges of the wall are restrained; (re): the wall is restrained with return walls.

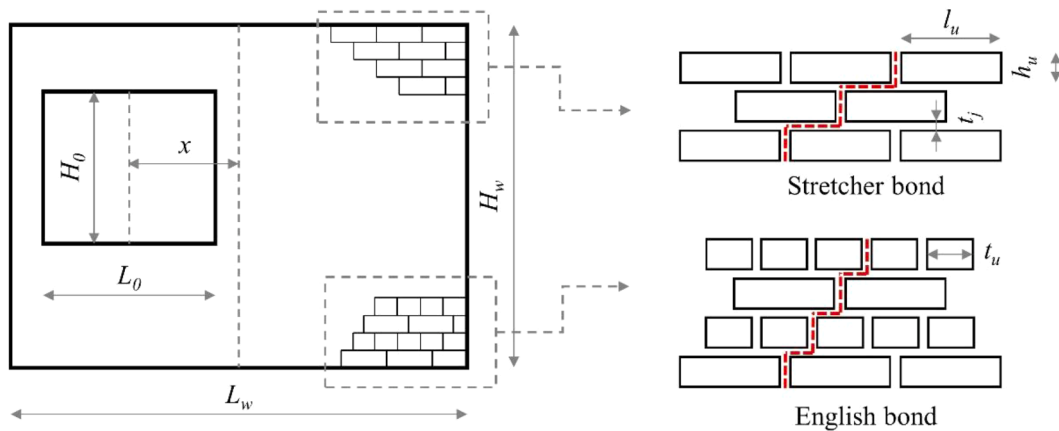


Fig. 2. The testing configuration of the testing specimens.

$$\alpha = \frac{GL_d}{H_d} \tag{5}$$

where  $H_d$  and  $L_d$  are the design height and design length of the wall, respectively. If the top edge of the wall is unsupported, the design height is the height of the wall ( $H_d = H_w$ ); otherwise, the design height is half of the height of the wall ( $H_d = H_w/2$ ). If one of the vertical edges is unsupported, the design length is the length of the wall ( $L_d = L_w$ ); otherwise, the design length is half of the length of the wall ( $L_d = L_w/2$ ); if an opening is presented,  $L_d$  is the length of the longer panel beside the opening.  $G$  is the assumed slope of the crack line;  $\alpha$  is the slope factor that identifies the expected cracking pattern including a vertical central crack in the case  $\alpha < 1$ , or a horizontal central crack in the case  $\alpha \geq 1$ ;  $\alpha_f$ ,  $k_1$  and  $k_2$  are coefficients determined by the presence of the openings, the slope factor  $\alpha$  and the number of supported vertical edges. Specifically,  $k_1$  is additionally determined by the restraint factor of vertical boundaries of the wall,  $R_f$ , which ranges from 0 (hinged) to 1 (clamped);

Table 2  
Percentage of incorrect predictions for the considered dataset.

Analytical formulations		EC6	AS3700	W2006	G2019
Incorrect overestimation	With opening	34.8%	10.9%	2.2%	2.2%
	Without opening	13.0%	10.9%	0.0%	4.3%
Incorrect underestimation	With opening	2.2%	17.4%	39.1%	34.8%
	Without opening	8.7%	17.4%	30.4%	23.9%
Incorrect prediction		58.7%	56.6%	71.7%	65.2%

$M_h$  and  $M_d$  are the horizontal and the diagonal bending moment capacity of masonry, respectively.

For the horizontal bending moment capacity ( $M_h$ ) and diagonal bending moment capacity ( $M_d$ ), AS3700 adopts the following equations:

$$M_h = \text{the least of } \begin{cases} 2\phi \cdot k_p \left( \sqrt{f_{x1}} \right) \left( 1 + \frac{\sigma_d}{f_{x1}} \right) Z_d \text{ (stepped failure)} \\ 4\phi \cdot k_p \left( \sqrt{f_{x1}} \right) Z_d \text{ (stepped failure)} \\ \phi \left( 0.44f_{bi}Z_u + 0.56f_{x1}Z_p \right) \text{ (line failure)} \end{cases} \tag{6}$$

$$M_d = \phi \left( 2.25\sqrt{f_{x1}} + 0.15\sigma_d \right) Z_t \tag{7}$$

$$k_p = \text{the least of } \begin{cases} s_p/t_u \\ s_p/h_u \\ 1 \end{cases} \tag{8}$$

where  $\phi$  is a capacity reduction factor;  $s_p$  is the minimum overlap of masonry units in successive courses;  $k_p$  is the perpend spacing factor, for stretcher bond,  $k_p = 1$ ;  $Z_d$ ,  $Z_u$  and  $Z_p$  are section modulus of bedded area, section modulus of masonry unit and section modulus of the perpend joints, respectively;  $Z_t$  is the equivalent torsional section modulus. Besides, it is worthy to note that  $M_h$  in stepped failure cases is dimensionally inconsistent. In this paper the capacity reduction factor is set to unity, because mean value of material properties are considered for comparison with the testing data.

For W2006 and G2019, the following equations are applied to compute  $M_h$  and  $M_d$ :

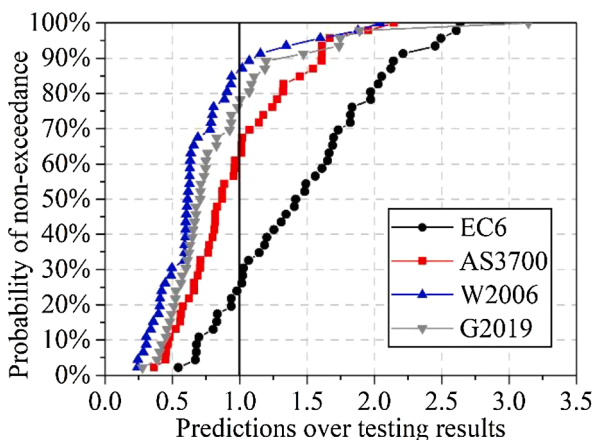


Fig. 3. Cumulative distribution function for ratios of the predictions over the testing results with partially clamped boundary conditions.

Table 3  
The average of predictions on all testing specimens by each formulation considering partially clamped boundaries.

Analytical formulations	EC6	AS3700	W2006	G2019
Average of predictions on all testing specimens	147%	98%	71%	85%
CV	0.38	0.43	0.55	0.59
N( $\pm 20\%$ )*	12	17	8	12

\* N( $\pm 20\%$ ) denotes the number of predictions that deviates from the testing results no more than 20%.

Table 4  
Ratio of predictions with clamped edges to those with hinged edges on average of all testing specimens.

Analytical formulations	EC6	AS3700	W2006	G2019
$W_{clamped}/W_{hinged}$	196%	201%	232%	219%

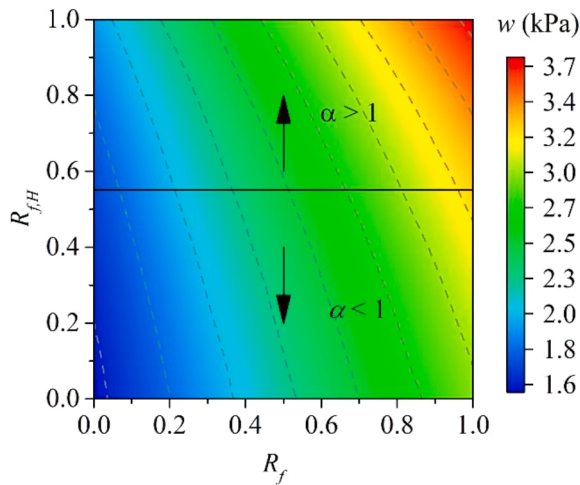


Fig. 4. Sensitivity study with regard to  $R_f$  and  $R_{f,H}$  based on TUD\_COMP-26 [17].

$$M_h = \text{lesser of} \begin{cases} \frac{1}{2(h_u + t_j)} \left[ (f_{bt} - \nu \cdot \sigma_d) h_u \cdot \frac{t_u^2}{6} \right] & (\text{line failure}) \\ \frac{1}{h_u + t_j} [\tau_u k_b \cdot 0.5 (l_u + t_j) t_u^2] & (\text{stepped failure}) \end{cases} \quad (9)$$

$$M_d = \frac{\sin \varphi}{h_u + t_j} \left[ (\sin \varphi)^3 \tau_u k_b + \frac{(\cos \varphi)^3 (f_{x1} + \sigma_d)}{6} \right] \cdot 0.5 (l_u + t_j) t_u^2 \quad (10)$$

$$\varphi = \tan G \quad (11)$$

where  $\nu$  is the Poisson's ratio of masonry;  $k_b$  equalling to 0.213 is a coefficient for computing the torsional shear capacity of the bed joints [28];  $\tau_u$  is the ultimate torsional shear strength of masonry in bed joints;  $\varphi$  is tangent of the assumed slope of the crack line  $G$ .

For  $\tau_u$ , W2006 adopts the following equation:

$$\tau_u = 0.9\sigma_d + 1.6f_{x1} \quad (12)$$

while G2019 adopts the following equation:

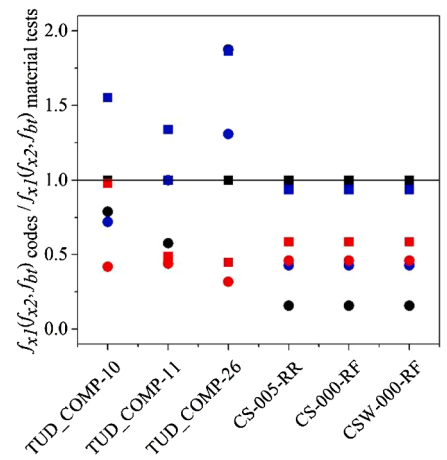
$$\tau_u = \begin{cases} 1.14\sigma_d + 1.81 & (\text{for CS brick masonry}) \\ 1.55\sigma_d + 1.07 & (\text{for clay brick masonry}) \end{cases} \quad (13)$$

The only difference between G2019 and W2006 is the evaluating method on the torsional strength of the bed joints. The equation provided in G2019 was derived from a single testing campaign performing torsional strength tests on CS and clay brick masonry. Though in this paper G2019 was attempted to be compared with other formulations, its application to other testing campaigns may have limitations and results should be interpreted with care.

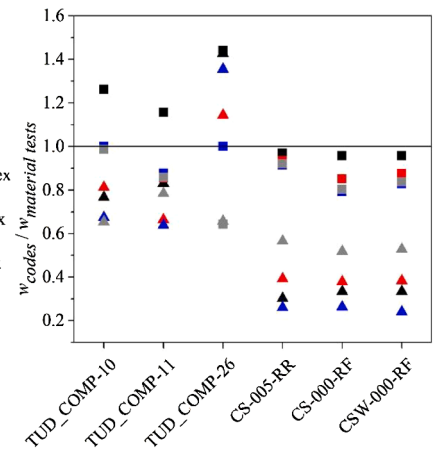
Mean values of material properties were adopted in the analytical calculations. When the material properties were not provided in the companion tests, the following procedure was adopted: where  $f_{bt}$  was not available, it was taken as 1/10 of the compressive strength of brick  $f_b$  [30]; where  $f_{x2}$  was not available,  $f_{x2}$  was calculated according to [31]:

$$f_{x2} = \text{lesser of} \begin{cases} \frac{1}{9} \left( 4 \frac{f_{bt}}{f_{x1}} + 5 \right) f_{x1} \\ \left( \frac{s_p}{t_u} \right)^2 \cdot \frac{2.75}{\sqrt{f_{x1}}} \cdot f_{x1} \end{cases} \quad (14)$$

Walls with openings are not covered in Annex E of EC6 [25]. For sake of simplicity, panels beside openings were considered as independent walls with one vertical side unsupported. The force capacity was determined as the minimum of the force capacity of the entire wall without the opening and that of the longer panel beside the opening. These two scenarios have also been considered in the calculations with



(a) Material properties from material tests and codes



(b) Predictions using various sources of material properties

Fig. 5. Predictions for 6 testing specimens based on various sources of material properties [16,17,20].

the other formulations.

Since the English bond is not considered in AS3700, W2006 and G2019, Eq. (4) is modified to account for potential slope of cracking line as shown in Fig. 2:

$$G = \frac{2(h_u + t_j)}{t_u + t_j} \quad (15)$$

### 3. General comparison of the analytical predictions against the testing results

To compare the accuracy of the formulations, the tested force capacity from the dataset presented in Section 2.1 was predicted according to the equations described in Section 2.2. Lower and upper bounds for each testing specimen were calculated. The lower bound of the force capacity was estimated by considering the wall hinged on all sides in EC6 or assuming  $R_f = 0$  in the other formulations; the upper bound of the force capacity was estimated by considering the wall clamped on all sides in EC6 or assuming  $R_f = 1$  for the other formulations.

Table 2 lists the percentage of incorrect predictions for each analytical formulation. For each testing specimen, if the tested force capacity was not comprised between the upper and lower bounds, the analytical prediction was defined as incorrect. More specifically, if the lower bound was higher than the testing result, an incorrect over-estimation was marked; if the upper bound was lower than the testing

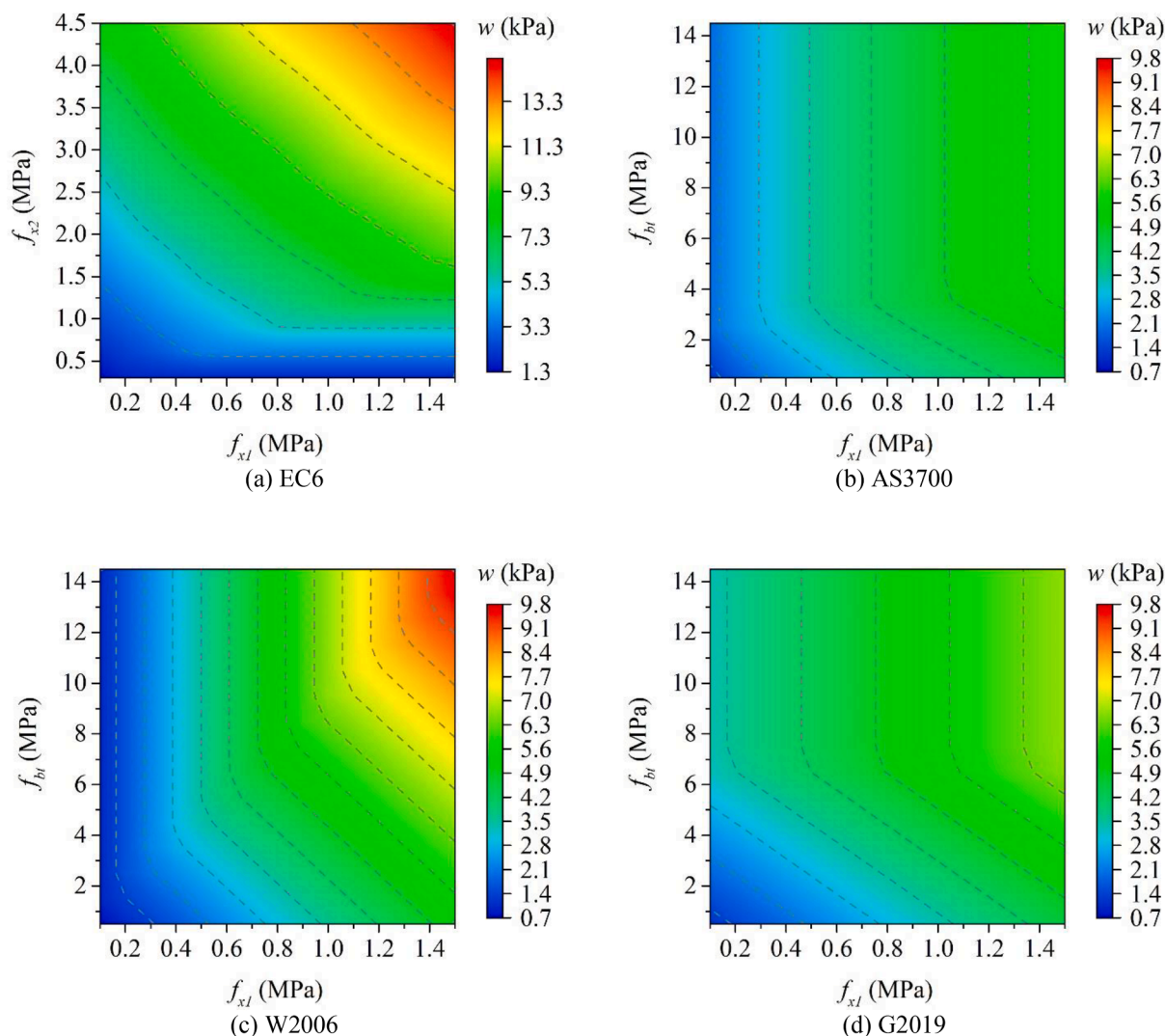


Fig. 6. Sensitivity study with regard to material properties based on TUD\_COMP-26 (without opening) [17].

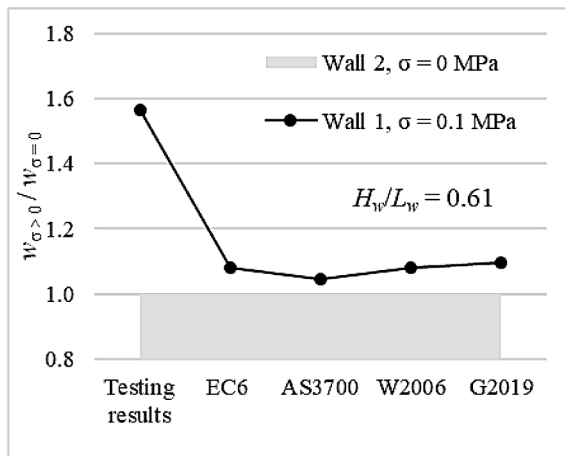
result, an incorrect underestimation was marked. The comparison shows that EC6 has an incorrect prediction rate of 58.7% with the highest overestimation rate of 47.8%. The proposed tactic to account for opening does not provide accurate results considering that EC6 provides more incorrect predictions for walls with openings compared with those without openings. W2006 and G2019 have incorrect prediction rates of 71.7% and 65.2%, respectively. Both these two formulations tend to underestimate the force capacity. AS3700 provides the lowest incorrect prediction rate of 56.6%. Also, the incorrect prediction rate on walls without openings of AS3700 is the lowest. Nevertheless, the accuracy of AS3700 requires further improvement considering 21.8% and 34.8% of testing specimens are overestimated and underestimated, respectively. The formulations based on the virtual work method provide close incorrect prediction rates for walls with and without openings.

Considering that nearly half of testing specimens were built with return walls, similar to constructions in practice, it is possible that partially clamped conditions are attained at the vertical supports. To examine the accuracy of the formulations considering the walls as partially clamped, the values of the lower and upper bounds were averaged in case of EC6, whereas  $R_f$  equalling to 0.5 was assumed for AS3700, W2006 and G2019. Here it is worthy to mention that  $R_f$  is essentially an indicator of not only the moment resistance contribution from vertical boundaries but also the overall crack propagation, as e.g. discussed in Ref. [32]. Fig. 3 shows the cumulative distribution function

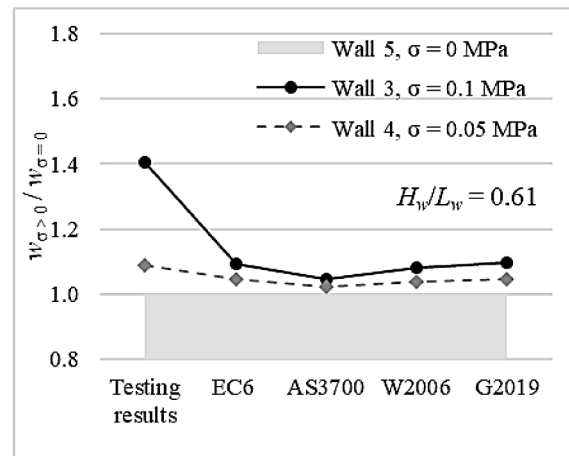
for the ratio of the predictions over the testing results. Provided that the ratio of a correct prediction over the testing result is 1 (marked with black line in Fig. 3), the probabilities of non-exceedance for the formulations from low to high are: 26% (EC6), 63% (AS3700), 78% (G2019) and 87% (W2006). This suggests that, when the walls are partially clamped, EC6 most possibly overestimates the force capacity, W2006 and G2019 tend to underestimate the force capacity, while AS3700 can provide the most close predictions.

Table 3 presents the average and the coefficient of variation (CV) of predictions on all testing specimens for each formulation considering the walls as partially clamped, where  $N(\pm 20\%)$  denotes the number of predictions that deviates from testing results no more than 20%. On average of all testing specimens, EC6 overestimates the force capacity up to 147%, which corresponds to previous observations. Both W2006 and G2019 underestimate the force capacity to 71% and 85% on average of all testing specimens, respectively; however, G2019 gives a higher  $N(\pm 20\%)$  value. AS3700 provides the closest prediction with an accuracy of 98% and the highest  $N(\pm 20\%)$  value. It can be concluded that within the listed dataset, AS3700 can be the most accurate of all analytical formulations evaluated in this paper, especially for partially clamped walls or walls with openings.

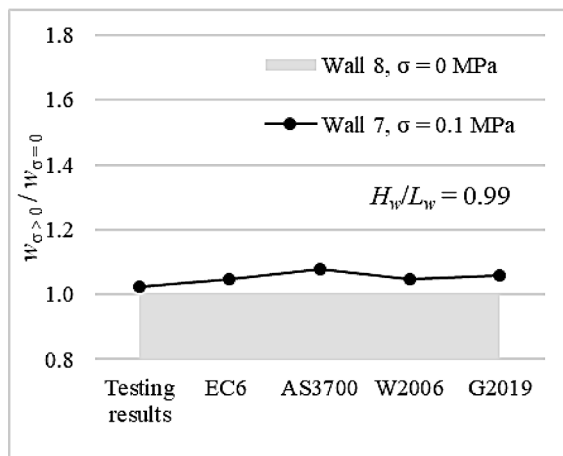
For detailed comparison regarding each specimen, the readers can refer to the Appendix.



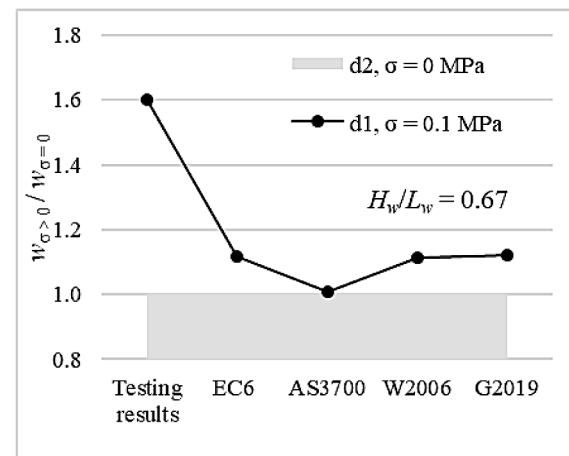
(a) Group 1 (without opening) [13]



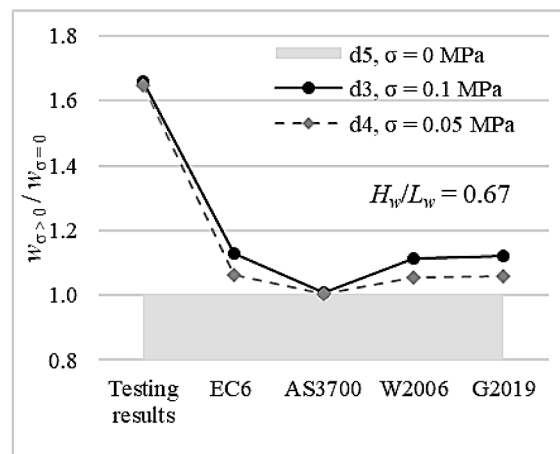
(b) Group 2 (with opening) [13]



(c) Group 3 (with opening) [13]



(d) Group 4 (without opening) [19]



(e) Group 5 (with opening) [19]

Fig. 7. Comparisons with regard to the pre-compression.

#### 4. Sensitivity study

In the following sections, the influence of the crucial factors on the force capacity will be studied individually. If not specifically mentioned, partially clamped vertical boundary conditions will be considered for the comparison between the testing results and the analytical predictions.

##### 4.1. Boundary conditions

The assumption of different boundary conditions can largely influence the estimation of the force capacity in current analytical formulations. Table 4 presents the ratio of predictions with clamped edges to those with hinged edges on average of all testing specimens for each formulation. All four formulations predict that with the same

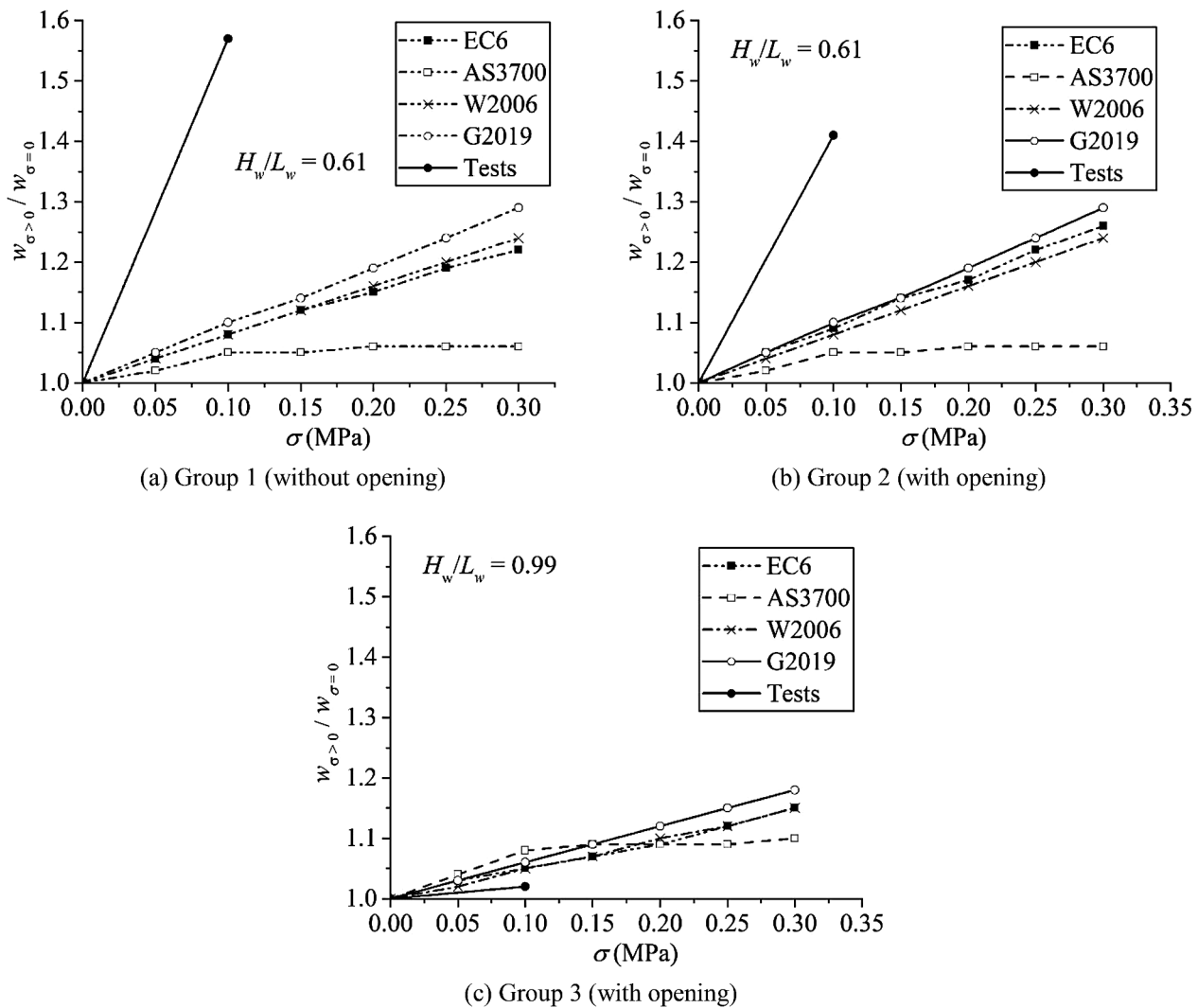


Fig. 8. Sensitivity study with regard to the pre-compression [13].

configuration, the force capacity of a wall can increase to around 200% as the boundary conditions change from hinged to clamped. Consequently, the parameters related to the vertical boundary conditions could be easily tuned to match testing results, which can result in overlooking the contribution of other parameters. Furthermore, the available testing campaigns provide limited information on the influence of different degree of restraint of the vertical boundary conditions. These together raise the importance and difficulty regarding studying the influence of the boundary conditions on the force capacity.

Apart from the vertical boundaries, contributions of horizontal boundary conditions, i.e., the top and bottom edges, were neglected in AS3700, W2006 and G2019. This treatment with horizontal boundary conditions can lead to an incorrect prediction on cracking pattern (related to the slope factor  $\alpha$ ) therefore leading to an inaccurate prediction on the force capacity [17]. Unlike testing specimens from other testing campaigns, the walls reported in Damiola et al. (2018) [17] show that diagonal cracks start a few courses away from the wall corners, which suggests higher degree of constraints at top and bottom edges. Considering that the virtual work method define the slope of diagonal cracks as starting from the wall corners, a mismatch between the predicted and the testing crack pattern is observed. In particular, a central vertical crack ( $\alpha < 1$ ) can be predicted instead of a central horizontal crack ( $\alpha > 1$ ), which results in an underestimation of the force capacity [17].

Based on previous discussions, a sensitivity study with AS3700 was

carried out to check both the influence of vertical and horizontal boundary conditions. Testing specimen TUD\_COMP-26 [17] was selected as reference. The wall is  $3950 \times 2710 \text{ mm}^2$ , four-side supported, without opening and made of clay brick masonry. Vertical edges were evaluated with the restraint factor  $R_f$ . A new coefficient  $R_{f,H}$  ranging from 0 to 1 was defined to take rotational stiffness of horizontal boundary conditions into account.  $R_{f,H}$  is used to define the calibrated design height  $H_d'$ , which replaces  $H_d$ , as described in the following equation:

$$H_d' = H_d - n \cdot h_u R_{f,H} \tag{16}$$

where  $n$  is the number of layers counted between the wall corner and the closest starting point of the diagonal crack.

Eq. (16) has the following physical meanings: when horizontal edges are simply hinged, i.e.  $R_{f,H} = 0$ , diagonal cracks start right at the wall corners; when horizontal edges are fully restrained, i.e.  $R_{f,H} = 1$ , diagonal cracks start  $n$  layers of bricks away from the wall corner. In this sensitivity study,  $n$  was assumed as 10 based on related testing observations [14,15]. It should be noted that  $R_{f,H}$  is not based on sufficient numbers of tests, but it is specified here to study the possible influence of horizontal boundary conditions based on AS3700.

Fig. 4 shows that the force capacity increases as  $R_f$  or  $R_{f,H}$  increases. This is partially inconsistent with the current formulation of AS3700 which suggests that horizontal boundaries have no contribution to the force capacity. Even so,  $R_f$  does have a larger influence than  $R_{f,H}$  on the

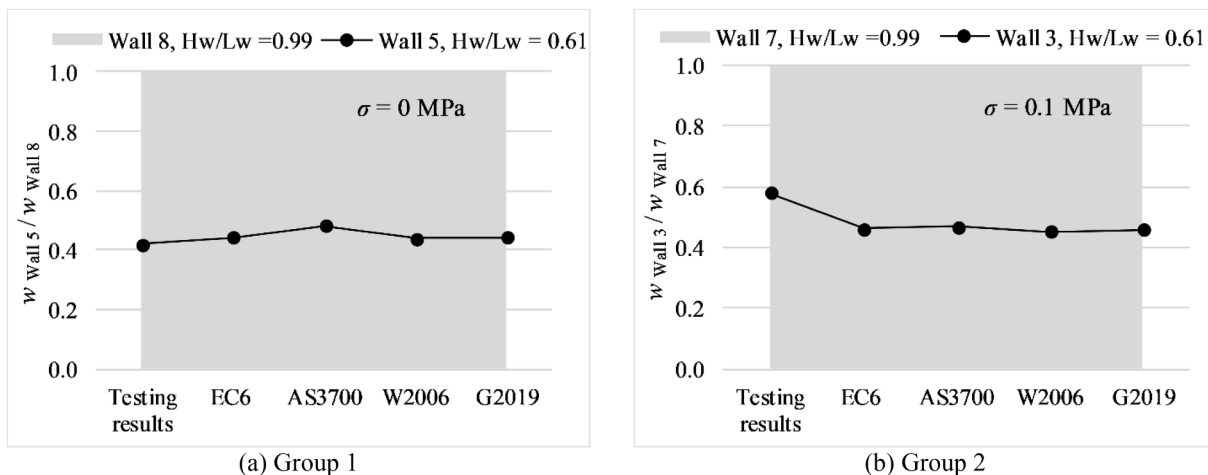


Fig. 9. Comparisons with regard to the aspect ratio [13].

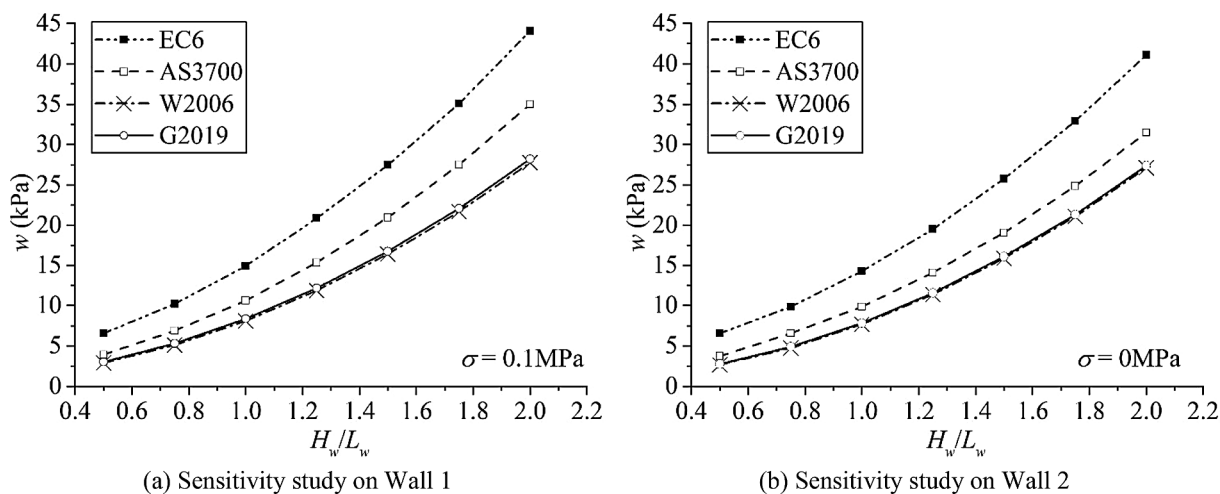


Fig. 10. Sensitivity study with regard to the aspect ratio [13].

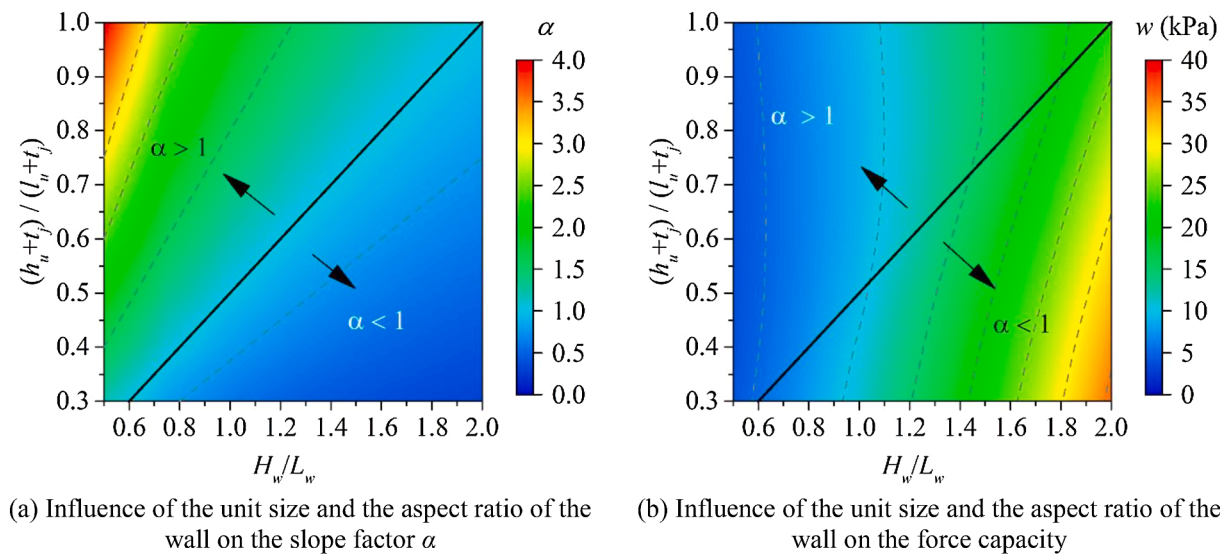


Fig. 11. Sensitivity study with regard to the unit size and the aspect ratio on Wall 1 [13].

**Table 5**  
Grouped testing specimens with regard to openings.

Groups	Testing specimens	Opening Area (%)	Opening eccentricity	Lateral pressure (kPa)	Reaction force (kN)	Predictions			
						EC6 (kPa)	AS3700 (kPa)	Willis 2006 (kPa)	Graziotti 2019 (kPa)
Group 1	SB01	–	–	2.80	38.91	2.25	1.56	1.14	1.30
	SB02	18%	Centric	2.40	27.25	2.25	1.10	0.82	0.93
	SB03	11%	Centric	2.30	28.42	2.25	1.07	0.83	0.94
	SB04	13%	Centric	2.20	26.52	2.25	1.24	0.88	1.00
Group 2	SB06	–	–	7.50	53.29	8.59	6.10	4.43	4.99
	SB07	11%	Centric	5.50	34.62	8.59	4.51	3.30	3.72
Group 3	DC01	–	–	2.65	36.83	3.19	3.04	1.60	1.11
	DC02	18%	Centric	1.75	19.87	3.19	2.32	1.21	0.86
Group 4	HW01	–	–	3.70	24.73	7.31	3.23	2.92	2.72
	HW02	4%	Centric	2.80	18.02	7.31	6.01	5.71	5.29
	HW03	8%	Centric	3.30	20.31	7.31	6.45	6.20	5.73
	HW04	7%	Centric	3.70	22.94	7.31	5.97	5.92	5.45
Group 5	Wall 1	–	–	4.76	47.00	8.68	5.13	3.80	3.96
	Wall 3	12%	Eccentric	5.05	44.20	6.79	3.34	2.47	2.58
Group 6	Wall 2	–	–	3.04	30.00	8.02	4.89	3.51	3.61
	Wall 5	12%	Eccentric	3.59	31.40	6.22	3.19	2.29	2.35
Group 7	TUD_COMP-11	–	–	2.45	27.00	2.49	2.89	1.55	2.93
	TUD_COMP-12	26%	Eccentric	3.67	22.40	2.49	1.93	1.05	1.94
Group 8	d1	–	–	3.95	8.96	5.60	4.02	2.49	2.96
	d3	13%	Eccentric	2.67	5.25	4.53	2.71	1.68	1.99
Group 9	d2	–	–	2.47	5.60	5.01	3.99	2.24	2.65
	d5	13%	Eccentric	1.61	3.16	4.02	2.69	1.51	1.78
Group 10	CS-000-RF	–	–	2.65	29.00	3.47	3.30	2.36	2.45
	CSW-000-RF	27%	Eccentric	2.34	18.80	3.47	1.62	1.17	1.23

force capacity. As  $R_f$  increases from 0 to 1, the force capacity increases by 90%, while as  $R_{f,H}$  increases in the same range, the force capacity increases by 30%. The slope factor  $\alpha$  equalling to 1 is marked with a solid black line in the graph. In fact,  $\alpha$  is not related to  $R_f$ , but increases as  $R_{f,H}$  increases. As  $R_{f,H}$  increases, an assumed central vertical crack ( $\alpha < 1$ ) would turn to an assumed central horizontal crack ( $\alpha > 1$ ) which leads to a larger estimated force capacity. The results stand also for W2006 and G2019 since they evaluate the boundary conditions in the same way as AS3700 does.

The results above imply that the force capacity predicted by the virtual work method is sensitive to the boundary conditions, especially the vertical ones, and to the assumed cracking patterns. Hence, a detailed study on the estimation of the  $R_f$  values for different vertical boundary conditions is necessary. Additionally, further investigations regarding the influence of horizontal boundaries on cracking patterns are also suggested.

#### 4.2. Material properties

Material properties, such as the flexural strength of masonry  $f_{x1}$ ,  $f_{x2}$  and flexural strength of units  $f_{bt}$  are crucial input parameters for the analytical formulations. Generally, these parameters should be evaluated with dedicated companion material tests [27,33] which, however, are often lacking or incomplete in the considered testing campaigns. Additionally, the material characterisation can often not be performed for existing structures, especially regarding  $f_{x2}$ . In this case, mean properties may be estimated by related codes (e.g. [32,33]). Therefore, it is important to evaluate the sensitivity of analytical formulation to material properties and further examine the use of property values provided by codes.

Fig. 5 presents predictions for 6 testing specimens representing Dutch masonry [16,17,20] using values of material properties from material tests, the Dutch Annex to Eurocode 6 [31] and NPR 9998 [30]. For NPR 9998 the values from the category “clay bricks with mortar for general purpose (post 1945)” [30] were selected. For each formulation, ratios of predictions with values recommended in codes ( $w_{codes}$ ) over those with values from material tests ( $w_{material\ tests}$ ) are presented. Fig. 5a shows that the estimations of material properties by codes can have large differences with those from material tests. Fig. 5b shows that, in

most cases, the predictions obtained using property values from codes, especially NPR 9998, can be over conservative compared to those using values from the material tests. On the opposite, several predictions according to EC6 using values from the Dutch Annex to Eurocode 6 are even higher than those using values from material tests. Overall, there can be large differences between predictions that adopt material properties from tests and those that use values recommended in codes. This suggests that in practice misevaluating the material properties can result in misevaluating also the force capacity to a large degree.

A sensitivity study was carried out to evaluate the influence of material properties on the force capacity estimated by the analytical formulations. According to Eqs. (2), (6) and (10),  $f_{x1}$  and  $f_{x2}$  are two material properties used in EC6, while  $f_{x1}$  and  $f_{bt}$  are required for the other formulations. In this sensitivity study,  $f_{x1}$ ,  $f_{x2}$  and  $f_{bt}$  have a range of 0.1–1.5 MPa, 0.3–4.5 MPa and 0.5–14.5 MPa, respectively. TUD\_COMP-26 (without opening) [17] was selected as reference. The sensitivity study mainly considered common cases within the range of the dataset in which  $f_{bt}$  is larger than or close to  $f_{x1}$ .

Fig. 6 shows the evaluated force capacity considering various combinations of material properties. According to EC6, the force capacity increases with the increase of  $f_{x2}$ , while the force capacity is not influenced by  $f_{x1}$  when  $f_{x2}$  is relatively small. The latter results derive from the fact that when the apparent vertical bending strength ( $f_{x1} + \sigma_d$ ) is larger than  $f_{x2}$ , the flexural strength ratio  $\mu$  will be limited to the unity. In this case, the force capacity is insensitive to  $f_{x2}$  (see Eqs. (1) and (2)). Fig. 6b–d show that with AS3700, W2006 and G2019, the force capacity increases with the increase of  $f_{x1}$ , while  $f_{bt}$  has a limited influence. Indeed, if  $f_{bt}$  is far larger than  $f_{x1}$  ( $f_{bt} \gg f_{x1}$ ), the horizontal bending capacity  $M_h$  is determined by stepped failure (Eqs. (6) and (9)). In this case, the increase of  $f_{bt}$  will not lead to an increase of the force capacity. Further comparing Fig. 6c and d, it shows that  $f_{bt}$  has a larger influencing area in W2006 than that in G2019. This is because in W2006  $M_h$  (stepped failure) is dependent on  $f_{x1}$ . Hence, the boundary where stepped failure changes into line failure is variable. In contrast, in G2019  $M_h$  (stepped failure) is independent on  $f_{x1}$ , therefore, the boundary where stepped failure changes into line failure is consistent. Nevertheless, with G2019 this result is influenced by the defined Eq. (13) of the torsional strength that does not explicitly consider the dependency of the torsional strength on the flexural strength of masonry as W2006 does.

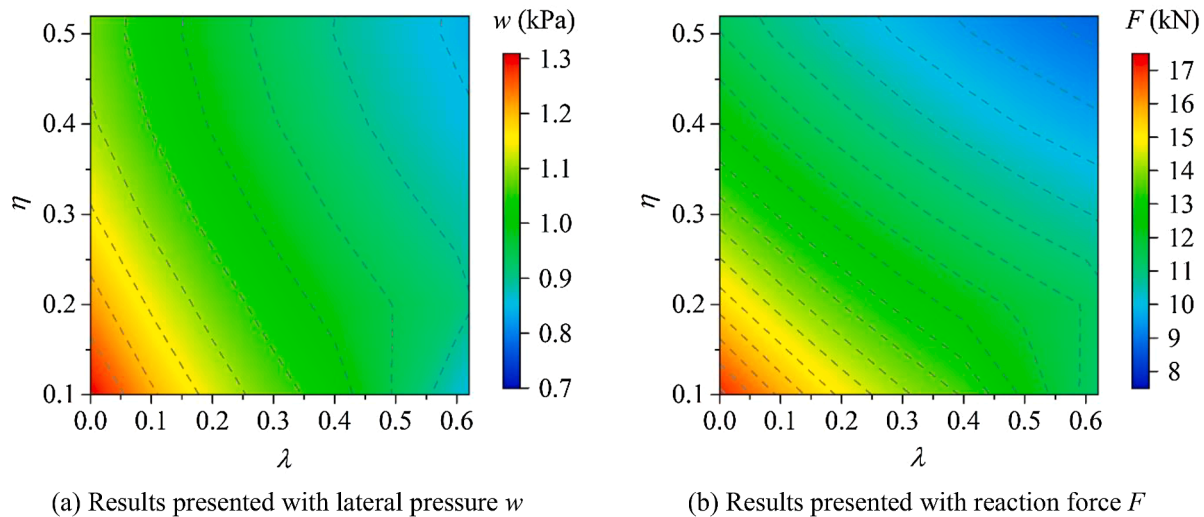


Fig. 12. Sensitivity study with regard to openings based on Group 1 [9].

Besides, the equation was derived only from a single testing campaign, and observations are not suggested to be generalised. Moreover, when using the same values of material properties, the predictions of formulations using the virtual work method vary from each other to a large degree. However, due to lack of related tests, it cannot be determined which formulation quantifies the influence of material properties correctly. This highlights the need of specific studies on the influence of material properties, especially torsional strength of joints.

### 4.3. Pre-compression

To examine how the formulations evaluate the influence of the pre-compression under different wall configurations, testing specimens were selected and divided in five groups [13,19]. In each group, testing specimens share the identical testing configuration, such as the wall geometry, boundary conditions and loading pattern, except for the pre-compression. Groups 1 and 4 do not have openings, while Groups 2, 3 and 5 have. The walls in Groups 1, 2, 4 and 5 have an aspect ratio around 0.6, while in Group 3 they have an aspect ratio around 1. Further discussion on the influence of aspect ratio and openings is presented in the following sections.

In Fig. 7, the markers represent the ratios of the force capacity of walls under pre-compressions over that under no pre-compression. The testing results show that for walls with aspect ratio 0.61–0.67 (Group 1, 2, 4 and 5), the ratio of the force capacity of the walls subjected to 0.1 MPa pre-compression over that of the walls under no pre-compression is approximately 1.5. In contrast, this comparing ratio drops to 1.02 for the walls with an aspect ratio close to 1 (Group 3). This suggests that the pre-compression has an obvious influence on the force capacity in case of walls with lower aspect ratios, while it has a limited influence on walls with larger aspect ratios. None of the formulations is able to predict this tendency for walls with small aspect ratios. Differently, for walls with larger aspect ratio (Fig. 7c), all formulations provide close predictions. Additionally, the testing results show that the force capacity of the wall subjected to an intermediate pre-compression (0.05 MPa) is also larger than that of the wall under no pre-compression. However, the increase in

the force capacity has a variation in a wide range between 10% and 60% (Fig. 7b, e). This requires for further testing to quantify the influence of pre-compression.

To further evaluate the influence of the pre-compression  $\sigma$  on the force capacity estimated by formulations, a sensitivity study was conducted referring to Group 1, 2 and 3 [13], with the values of  $\sigma$  ranging from 0 to 0.3 MPa. Fig. 8a, b show that according to the formulations, when the aspect ratio is relatively small (0.61), the force capacity increases slightly as  $\sigma$  increases, no matter if an opening is present; when the aspect ratio is relatively large (0.99), the increase of the force capacity with regard to  $\sigma$  is similar as observed from tests. In general, the force capacity predicted by AS3700 is less sensitive to the change of the pre-compression, while the force capacity predicted by the other formulations increases linearly but slightly as the pre-compression increases.

### 4.4. Aspect ratio

Section 4.3 reveals interdependency between the influence of the aspect ratio of the wall ( $H_w/L_w$ ) and the pre-compression on the force capacity. The aim of this section is to evaluate the aspect ratio of the walls at different levels of pre-compression. Due to lack of tests specifically studying the influence of aspect ratio, only two groups including 4 testing specimens were found (Walls 3, 5, 7 and 8) [13]. It should be noted that these four testing specimens are all with openings. The eccentricity and the area of the openings can influence the force capacity. Consequently, this comparison can provide only an indication of the trend rather than general conclusions.

In Fig. 9, markers represent the ratios of the force capacity of walls with aspect ratios of 0.61 over those with aspect ratios of 0.99. The testing results show that if the pre-compression is 0.1 MPa, this comparing ratio is 0.58, while this ratio is 0.42 in the case of no pre-compression. This again suggests that the force capacity of the walls with lower aspect ratios can be lower than that of the walls with higher aspect ratios. Besides, all formulations can predict the enhancing effect of the increasing of the aspect ratio, however, they cannot apparently

Table 6 Comparison with regard to the wall thickness and the bonding pattern.

Testing specimens	Wythe	Bonding pattern	Wall thickness (mm)	Testing results (kPa)	EC6 (kPa)	$\alpha$	AS3700 (kPa)	W2006 (kPa)	G2019(kPa)
TUD_COMP-26	Single	Stretcher	100	3.37	2.27	0.80	2.23	1.38	3.33
TUD_COMP-27	Double	English	210	7.52	7.74	1.55	3.40	7.08	23.65
URM-F	Double	English	229	19.26	16.00	1.38	9.27	25.89	33.65

predict the influence of the change of the pre-compression, as observed in Section 4.3.

A sensitivity study based on Wall 1 and Wall 2 (without openings) [13] was carried out to evaluate the influence of  $H_w/L_w$  ranging from 0.5 to 2. Fig. 10 shows that according to the formulations, the force capacity increases non-linearly as  $H_w/L_w$  increases. All formulations predict similar tendencies. Similarly to what observed in Section 4.3, the analytical predictions predict that the pre-compression has only a slight influence on the force capacity (Fig. 10).

For the formulations based on the virtual work theory, the aspect ratio of the wall  $H_w/L_w$ , and the ratio of the unit  $(h_u + t_j)/(l_u + t_j)$  influence the estimation of the force capacity via the slope factor  $\alpha$  (Eq. (5)). Fig. 11 shows a sensitivity study considering the combined effects of  $H_w/L_w$  and  $(h_u + t_j)/(l_u + t_j)$  on Wall 1 with AS3700; the solid black line marks the case of  $\alpha$  equals to unity. Fig. 11b shows that the force capacity is sensitive to  $H_w/L_w$  as displayed in Fig. 10. In contrast, the force capacity is more sensitive to  $(h_u + t_j)/(l_u + t_j)$  in the case  $\alpha < 1$  than in the case  $\alpha$  greater than 1 when a central horizontal crack is assumed.

#### 4.5. Openings

To evaluate the application range of the formulations with regard to walls with openings, 10 groups of testing specimens were compared [9,13,17,19,20]. In each group, the first testing specimen is without opening, while the others are with openings, as reported in Table 5. Openings in Group 1–4 are centrally located, while in Group 5–10 they are eccentrically located. Table 5 shows that generally, the presence of openings weakens the force capacity measured in terms of lateral pressure. The walls in Group 5, 6 and 7 do not show this trend. This is because the lateral pressure was calculated by dividing the reaction force with the net area of the wall. The relatively smaller net area of the wall with opening can result in an unexpected higher force capacity. In this sense, in Group 5 and 7 the presence of the openings still weakens the force capacity, considering that the reaction forces of the walls without openings are higher than those of the walls with openings in the same group. The only exception is Group 6, where the reaction force of the wall without opening is instead slightly lower than its counterpart (30kN to 31.4kN).

By comparing the predictions with the testing results, Table 5 shows that for most cases, especially for walls with centric openings, the proposed simplified method based on Annex E of EC6 to account for openings does not provide satisfactory results. As described in Section 2.2, the proposed method for EC6 estimate the wall capacity by considering the minimum between the capacity of the wall without any opening and the capacity of the longer panel beside the opening treated as independent wall with one vertical side unsupported. According to Eq. (1), this resulted in the capacity of the panel being larger than that of the entire wall without opening in most of cases. Consequently, no distinction is made in the estimation of the capacity for walls with and without openings (e.g. Group 1–4).

In contrast to Annex E of EC6, the formulations based on the virtual work method take the openings into account. Similar to EC6, the force capacity predicted by these formulations was determined as the minimum of the force capacity of the entire wall without the opening and that of the longer panel beside the opening. In particular, the presence of the opening affects the estimation of coefficients  $k_1$ ,  $k_2$ , of the design length of the wall  $L_d$ , and of the aspect factor  $\alpha_f$  [27]. Similar to the testing results, most predictions return that the openings weaken the force capacity. An exception is Group 4, where the force capacity of the wall with opening is larger that of its counterpart. This is because the design length  $L_d$  of the wall with opening is so small that it results in a relatively large force capacity.

A sensitivity study was carried out to check the influence of the openings on the force capacity based on Group 1 [9] considering AS3700. The walls are  $5615 \times 2475 \text{ mm}^2$ , top-free and made of clay brick masonry. The eccentricity and the length of the opening were

considered as variables. The consideration of the length instead of the area of the opening lies in the fact that in AS3700, the height of the opening is not considered. Normalised geometrical parameters are introduced as following:

$$\lambda = \frac{x}{\left(\frac{L_w - L_o}{2}\right)} \in [0, 62] \quad (17)$$

$$\eta = \frac{L_o}{L_w} \in [0.1, 0.52] \quad (18)$$

where  $x$  is defined as the distance between the central line of the opening and that of the wall;  $L_w$  and  $L_o$  are the length of the wall and the length of the opening, respectively (Fig. 2);  $\lambda$  is the normalised variable representing the eccentricity of the opening;  $\eta$  is the normalised variable representing the length of the opening. Ranges of  $\lambda$  and  $\eta$  are determined as those covering all testing specimens ( $\eta$  does not start from 0 to avoid calculating error). This is intended to provide a reference for practical configurations of the openings.

Fig. 12 shows the variation of the force capacity in terms of pressure ( $w$ ) and force ( $F$ ) at varying  $\lambda$  and  $\eta$ . Results show that the further the opening is positioned away from the central line of the wall ( $\lambda$  from 0 to 0.62), the smaller the force capacity; the force capacity decreases as the length of the opening increases ( $\eta$  from 0.1 to 0.52) except for a small area where  $\eta$  is  $< 0.2$  and  $\lambda$  is larger than 0.5. These results provide insights about how the formulations based on the virtual work method evaluate the influence of the openings. Nevertheless, tests are very limited concerning a detailed study on the influence of the eccentricity and the area of the openings. Therefore, the predictions by the formulations are not suggested to be generalized.

#### 4.6. Wall thickness/bonding patterns

Despite the presence of numerous multi-wythe walls in existing URM structures, the majority of testing campaigns (44 out of 46 testing specimens listed in this paper) focus on single-wythe walls built in stretcher bond. According to Annex E of EC6, walls to be evaluated should be solid walls with thickness less than or equal to 250 mm [25]. If the unit thickness is 100 mm, a triple-wythe wall is already beyond the applied range of the code. As for the other formulations, since the assumed cracking pattern is based on stretcher bond, their applications to multi-wythe walls are naturally limited.

In this section, testing specimen TUD\_COMP-26 and TUD\_COMP-27 are compared since the former is single-wythe and stretcher bonded, while the latter is double-wythe and English bonded. Apart from thickness and bonding pattern they have the same testing configurations. Different bonding patterns and wall thickness are here compared together since in practice the latter depends on the former. Additionally, the double-wythe wall URM-F tested by Padalu et al [18] is also considered to check the accuracy of formulations treating multi-wythe walls. Here the calculation for the slope factor  $\alpha$  related to assumed cracking pattern is adapted for English bond as shown in Eq. (15).

Table 6 shows that the force capacity of TUD\_COMP-27 measured in tests is 2.2 times than that of TUD\_COMP-26. It is not clear whether this enhancing effect is caused by the change of wall thickness or bonding pattern. Indeed, increasing the wall thickness increases the section modulus of the wall, while the transverse bricks in English bonded walls provide an interlocking effect between wythes. The formulations based on the virtual work method either underestimate the ratio of double-wythe wall to single-wythe wall (AS3700, 1.5) or extremely overestimate it (W2006, 5.2; G2019, 7.1). AS3700, W2006 and G2019 wrongly predict  $\alpha$  for TUD\_COMP-26. It should be noted that the horizontal boundary conditions can also play a role as discussed in Section 4.1. Considering absolute values, EC6 appears to be the most accurate. As for URM-F, EC6 again predicts the most accurate value, while the other 3 formulations either underestimate or overestimate the wall

capacity excessively. Calculated  $\alpha$  for URM-F is larger than 1, which is against the testing observation where a central vertical crack took place. This suggests that evaluation for English bonded and multi-wythe walls by AS3700, W2006 and G2019 should be further studied.

## 5. Conclusions

This paper evaluates the accuracy and application range of current major analytical formulations assessing the force capacity of unreinforced masonry (URM) walls in out-of-plane (OOP) two-way bending. For this purpose, 46 testing specimens from 8 international testing campaigns were collected and categorised. The formulation provided by Eurocode 6 (EC6) based on the yield line theory, and the formulations based on the virtual work method proposed by the Australian Standard (AS3700), Willis et al. (W2006), and Graziotti et al. (G2019) were considered.

The accuracy of the formulations was evaluated by comparing the predictions with the testing results. The comparison shows that AS3700 provides the highest predicting accuracy rate within the dataset. More specifically, AS3700 is the most accurate assessing walls assumed to be partially clamped and walls with openings. Even so, the incorrect prediction rate of AS3700 is as high as over 50%. EC6 tends to incorrectly overestimate the force capacity for most testing specimens. W2006 and G2019 tend to incorrectly underestimate the force capacity equally for walls with or without openings. Nevertheless, among the formulations based on the virtual work method, the approach proposed by Willis et al. (W2006) appears the one with the strongest theoretical framework to be employed for further improvements. The results obtained by G2019 should be treated with care, since the proposed equation for the torsional strength was derived from a single testing campaign and not meant to be generalised.

To evaluate the application range of formulations, the influence of the crucial factors on the force capacity was explored by comparing the available testing results and by performing sensitivity studies for the analytical formulations.

The influence of the boundary conditions was first evaluated. Study on the boundary conditions based on formulations shows that as a wall changes from hinged to clamped, its force capacity increases to about 200%. A sensitivity study based on AS3700 shows that the force capacity is not only sensitive to the rotational stiffness of the vertical boundaries, but also to the rotational stiffness of the horizontal boundaries, although to a smaller degree. This is contradictory with the assumption in the virtual work method. However, this finding requires further study due to limited testing evidence.

The lack of material characterisation for existing buildings often results in the need of adopting prescribed material properties, which generally leads to a misvaluation of the force capacity. In most cases, the predictions using values from codes, especially for NPR 9998, are over conservative compared to those using values from material tests. The sensitivity study shows that with EC6, the force capacity increases with the increase of horizontal flexural strength of masonry  $f_{x2}$ , while the force capacity is not influenced by vertical flexural strength of masonry  $f_{x1}$  if the horizontal one  $f_{x2}$  is relatively small. With AS3700, W2006 and G2019, the force capacity increases with the increase of the vertical flexural strength of masonry  $f_{x1}$ , while the flexural strength of bricks  $f_b$  has a limited influence. However, due to lack of related tests, it cannot be determined which formulation quantifies the influence of material properties correctly. Additionally, it is worthy to highlight the importance of characterising the torsional shear response of the bed joints, since it can significantly influence the evaluation of the wall capacity.

A study on the influence of the pre-compression shows that the pre-compression has an obvious enhancing effect on the force capacity of walls with relatively small aspect ratios. In contrast, this effect is quite slight for walls with relatively large aspect ratios. However, none of the formulations can correctly predict the influence of pre-compression for

walls with small aspect ratios. The influence of the aspect ratio of the wall was also examined. Both testing results and predictions show that the force capacity increases nonlinearly as the aspect ratio of the wall increases.

The testing results show that the presence of openings weakens the force capacity. A simple extension of Annex E in EC6, made by the authors by considering the longer panel beside the opening as an independent wall with one vertical edge unsupported, does not predict this tendency, especially when the opening is centrally located. In contrast, predictions by AS3700, W2006 and G2019 methods match well with the testing observations. A sensitivity study shows that the force capacity decreases as the eccentricity or the length of the opening increases. Nevertheless, these results are not suggested to be generalised since the continuous varying ranges of the eccentricity and area of the openings discussed in this sensitivity study lack corresponding testing evidence.

The influence of the wall thickness and bonding pattern was studied jointly. EC6 is the most accurate formulation assessing the influence of the thickness, even though the bonding pattern is not considered. Formulations based on the virtual work method require further improvements to account for a wider range of wall thickness and bonding patterns.

To conclude, the formulations based on the virtual work method returned the most accurate predictions for the testing specimens evaluated in this paper, especially for partially clamped walls and walls with openings. Nevertheless, drawbacks and limitations were revealed when analytical formulations were applied to assess the influence of crucial factors on the force capacity. First, the influencing trend of some crucial factors predicted by the analytical formulations is contradictory with the testing results, such as the pre-compression. Second, the application ranges of some crucial factors are limited or not well defined, such as the boundary conditions and the wall thickness / bonding patterns. Third, the influence of some crucial factors cannot be determined due to lack of testing evidence, such as the material properties, and the eccentricity and area of the openings. These in total decrease the accuracy and limit the application range of the analytical formulations. To improve the accuracy and application range of the analytical formulations, further study is suggested regarding the influence of above-mentioned crucial factors on the wall failure mechanisms and quantifying the relations between the force capacity and the crucial factors.

## Declaration of Competing Interest

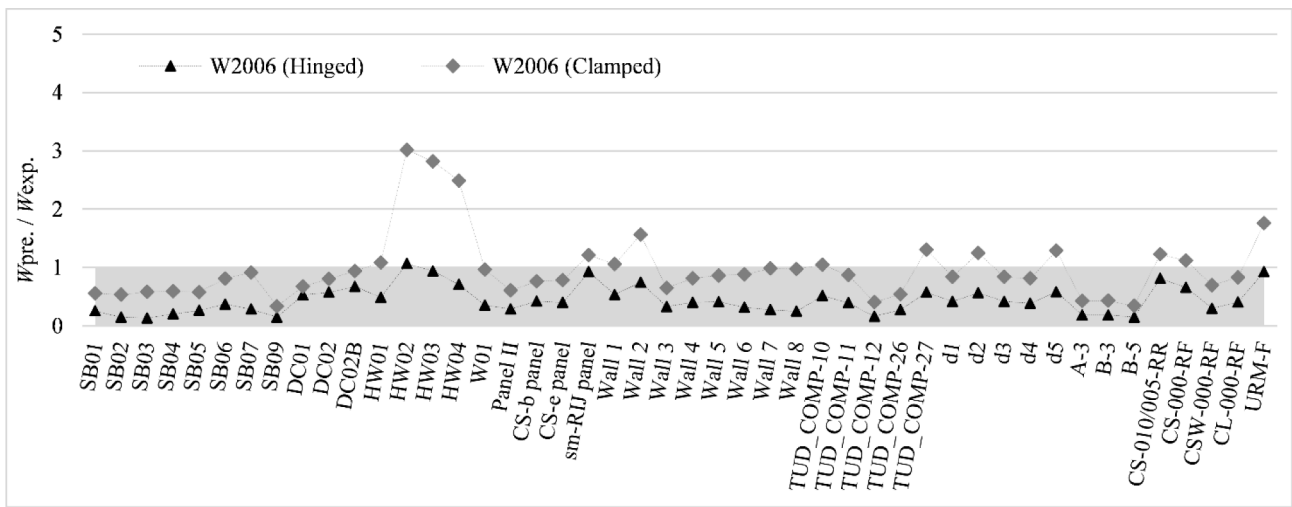
The authors declare that they have no known competing financial interests or personal relationships that could have appeared to influence the work reported in this paper.

## Acknowledgement

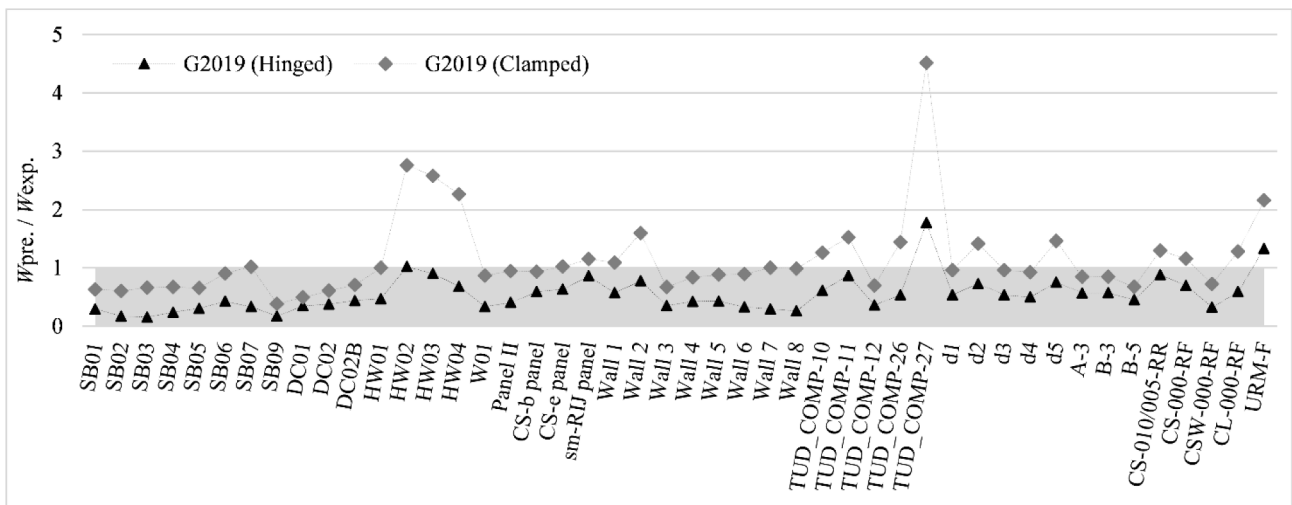
The financial support provided by the China Scholarship Council (CSC) to the first author is acknowledged. Besides, financial support from the Stichting Koninklijk Nederlands Normalisatie Instituut (NEN), under the contract 8505400026-001, is gratefully acknowledged. Special thanks go also to Prof. Jan Rots for his valuable advice.

## Appendix

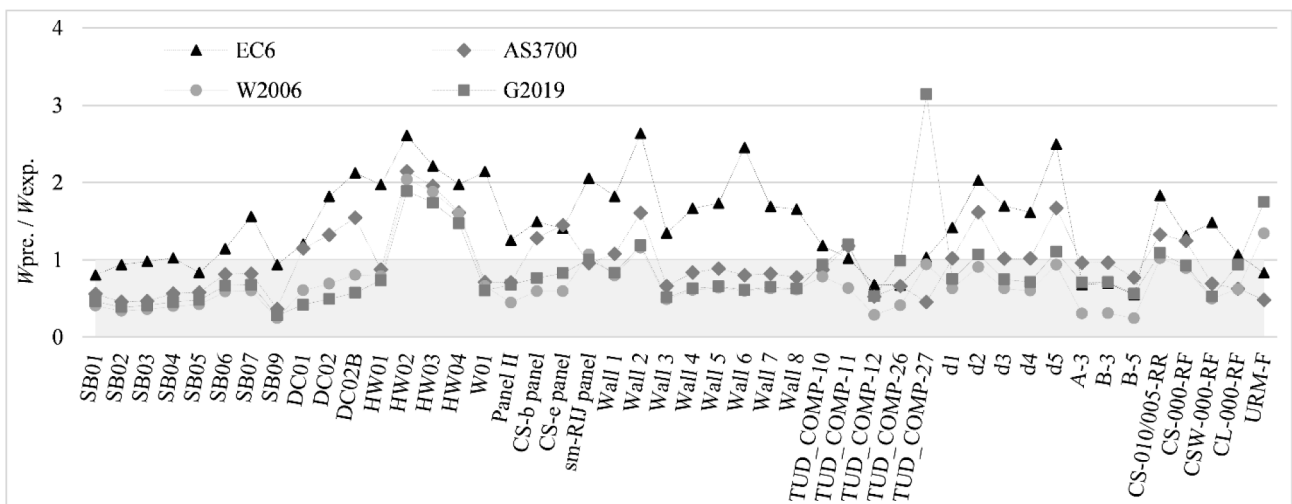
Detailed comparisons for all specimens corresponding to Section 3 are presented graphically as in Fig. 13. In Fig. 13a–d, the ratios between the predicted force capacity and the experimental one are reported considering hinged (black triangle markers) and clamped boundary conditions (grey rhombus markers). In Fig. 13e predictions considering specimens as partially clamped ( $R_f = 0.5$  for virtual work method formulations) are compared with the testing results.



(c) Predictions by W2006 versus the testing results



(d) Predictions by G2019 versus the testing results



(e) The testing results versus predictions by formulations considering the walls as partially clamped

Fig. 13. Graphical presentation of the detailed comparison between predictions and the testing results.

## References

- [1] D'Ayala DF, Paganoni S. Assessment and analysis of damage in L'Aquila historic city centre after 6th April 2009. *Bull Earthq Eng* 2011;9:81–104.
- [2] Moon L, Dizhur D, Senaldi I, Derakhshan H, Griffith M, Magenes G, et al. The demise of the URM building stock in christchurch during the 2010–2011 Canterbury Earthquake Sequence. *Earthq Spectra*. 2014;30:253–76.
- [3] Penna A, Morandi P, Rota M, Manzini CF, da Porto F, Magenes G. Performance of masonry buildings during the Emilia 2012 earthquake. *Bull Earthq Eng* 2014;12: 2255–73.
- [4] Sorrentino L, D'Ayala D, de Felice G, Griffith MC, Lagomarsino S, Magenes G. Review of out-of-plane seismic assessment techniques applied to existing masonry buildings. *Int J Archit Herit*. 2016;1–20.
- [5] Derakhshan H, Griffith MC, Ingham JM. Out-of-plane behavior of one-way spanning unreinforced masonry walls. *J Eng Mech*. 2013;139:409–17.
- [6] Derakhshan H, Dizhur DY, Griffith MC, Ingham JM. Seismic assessment of out-of-plane loaded unreinforced masonry walls in multi-storey buildings. *Bullet New Zealand Soc Earthquake Eng* 2014;47.
- [7] Walsh KQ, Dizhur DY, Almesfer N, Cummskey PA, Cousins J, Derakhshan H, et al. Geometric characterisation and out-of-plane seismic stability of low-rise unreinforced brick masonry buildings in Auckland, New Zealand. *Bullet New Zealand Soc Earthquake Eng* 2014;47.
- [8] Doherty K, Griffith MC, Lam N, Wilson J. Displacement-based seismic analysis for out-of-plane bending of unreinforced masonry walls. *Earthquake Eng Struct Dyn* 2002;31:833–50.
- [9] Chong VL. The behaviour of laterally loaded masonry panels with opening. Plymouth, UK: University of Plymouth; 1993.
- [10] van der Pluijm R. Report TUE-BCO\_9903: Test on laterally loaded clay brick panels. Eindhoven, the Netherlands: Eindhoven University of Technology; 1999.
- [11] van der Pluijm R. 2001-CON-BM-R5015: Laterally Loaded Masonry Panels made with Thin Layer Mortar. Delft, the Netherlands: TNO; 2001.
- [12] Derakhshan H, Lucas W, Visintin P, Griffith MC. Out-of-plane strength of existing two-way spanning solid and cavity unreinforced masonry walls. *Structures* 2018; 13:88–101.
- [13] Griffith MC, Vaculik J, Lam NTK, Wilson J, Lumantarna E. Cyclic testing of unreinforced masonry walls in two-way bending. *Earthquake Eng Struct Dyn* 2007; 36:801–21.
- [14] Ravenshorst GJP, Messali F. C31B60: Out-of-plane tests on replicated masonry walls. Delft, the Netherlands: Delft University of Technology; 2016.
- [15] Damiola M, Esposito R, Ravenshorst GJP. C31B67: Quasi-static cyclic out-of-plane tests on masonry components 2016/2017. Delft, the Netherlands: Delft University of Technology; 2017.
- [16] F. Messali G. Ravenshorst R. Esposito J.G. Rots Large-scale testing program for the seismic characterization of Dutch masonry walls 2017 Santiago, Chile 16WCEE.
- [17] M. Damiola R. Esposito F. Messali J.G. Rots Quasi-static cyclic two-way out-of-plane bending tests and analytical models comparison for URM walls 2018 Milan, Italy.
- [18] Padalu PKVR, Singh Y, Das S. Cyclic two-way out-of-plane testing of unreinforced masonry walls retrofitted using composite materials. *Constr Build Mater* 2020;238.
- [19] Vaculik J, Griffith MC. Out-of-plane shaketable testing of unreinforced masonry walls in two-way bending. *Bull Earthq Eng* 2017;16:2839–76.
- [20] Graziotti F, Tomassetti U, Sharma S, Grotoli L, Magenes G. Experimental response of URM single leaf and cavity walls in out-of-plane two-way bending generated by seismic excitation. *Constr Build Mater* 2019;195:650–70.
- [21] Griffith MC, Vaculik J. Out-of-plane flexural strength of unreinforced clay brick masonry walls. *TMS J* 2007;25:53–68.
- [22] Haseltine BA, Tutt JN, West HWH. The resistance of brickwork to lateral loading, part II: Design of walls to resist lateral loads. *J Inst Struct Eng* 1977;55:422–30.
- [23] B.P. Sinha Simplified ultimate load analysis of laterally loaded model orthotropic brickwork panels of low tensile strength *Struct Eng Part B*. 56 1978 B:81–4.
- [24] Hendry AW, Sinha BP, Davies S. Design of masonry structures. CRC Press 2017.
- [25] CEN. Eurocode 6: Design of masonry structures-Part 1-1: General rules for reinforced and unreinforced masonry structures. Comité Européen de Normalisation: Brussels, Belgium, 2012.
- [26] Lawrence S, Marshall R. Virtual work design method for masonry panels under lateral load. 12th International brick/block masonry conference. Madrid, Spain2000. p. 1063-73.
- [27] International Standard Australia. Australian standard for masonry structures AS 3700:2018. Sydney: Australia; 2018.
- [28] Willis CR, Griffith MC, Lawrence SJ. Moment capacities of unreinforced masonry sections in bending. *Aust J Struct Eng* 2006;6:133–46.
- [29] Vaculik J, Griffith MC. Out-of-plane load–displacement model for two-way spanning masonry walls. *Eng Struct* 2017;141:328–43.
- [30] NEN. NPR, 9998 - Beoordeling van de constructieve veiligheid van een gebouw bij nieuwbouw, verbouw en afkeuren Delft, the Netherlands 2018.
- [31] NEN. NEN-EN 1996-1-1 National Annex to Eurocode 6. Delft, the Netherlands, 2018.
- [32] Sharma S, Tomassetti U, Grotoli L, Graziotti F. Two-way bending experimental response of URM walls subjected to combined horizontal and vertical seismic excitation. *Eng Struct* 2020;219.
- [33] CEN. EN 1052-2 – Methods of test for masonry – Part 2: Determination of flexural strength. 1999.